

Gravity Anomaly Modeling of Sedimentary Basins by Means of Multiple Structures and Exponential Density Contrast-depth Variations: A Space Domain Approach

V. CHAKRAVARTHI, B. RAMAMMA, and T. VENKAT REDDY

Centre for Earth & Space Sciences, University of Hyderabad, Gachibowli, Hyderabad – 500 046

Email: vcvarthi@rediffmail.com

Abstract: An automatic modeling scheme is developed in the space domain to interpret the gravity anomalies of sedimentary basins, among which the density contrast decreases exponentially with depth. Forward modeling is realized in the space domain using a combination of both analytical and numerical approaches. A collage of vertical prisms having equal widths, whose depths are to be estimated, describes the geometry of a sedimentary basin. Initial depths of a sedimentary basin are predicted using the Bouguer slab formula and subsequently updated, iteratively, based on the differences between the observed and theoretical gravity anomalies until the modeled gravity anomalies mimic the observed ones. The validity and applicability of the method is demonstrated with a synthetic and two real field gravity anomalies, one each over the Chintalpudi sub-basin in India and the other over the San Jacinto graben, California. In case of synthetic example, the assumed structure resembles a typical intracratonic rift basin formed by normal block faulting and filled with thick section of sediments. The proposed modeling technique yielded information that is consistent with the assumed parameters in the case of synthetic structure and with the available/drilling depths in case of field examples.

Keywords: Gravity anomalies, sedimentary basins, exponential density contrast, automatic modeling.

INTRODUCTION

One of the important applications of the gravity method is to trace the boundaries of concealed basement structures across which the density varies significantly. Owing to the deficit in density of sediments in comparison to basement rocks, negative gravity anomalies are usually observed over sedimentary basins having a large thickness. The deduced Bouguer gravity anomalies, considered to have been made on topographic elevations, can be analyzed quantitatively for the structures of basement interfaces concealed under the sedimentary load. However, the interpretation of gravity anomalies for sub-surface density structure(s) is a non-unique problem, because different mass distributions at different depths can produce identical surface gravity anomalies (Blakely, 1995). The ambiguity in gravity interpretation is often tackled by assigning a mathematical geometry to the anomalous mass with a known density and then to invert the anomalies for the unknown parameters (Murthy, 1998; Chakravarthi and Sundararajan, 2006a).

The mathematical geometries often used in sedimentary basin modeling are the stacked prism model of Bott (1960) and the polygonal model of Talwani et al. (1959). In the

Bott's (1960) method of gravity interpretation, the cross-section of a sedimentary basin was described with a series of juxtaposed vertical prisms having equal widths, whereas, in the method of Talwani et al. (1959), the outline of the basin was approximated by an N-sided polygon. Although many forward modeling schemes (e.g., Won and Bevis, 1987; Singh, 2001) to compute the theoretical gravity anomalies are available, they are of limited application in analyzing the gravity anomalies of sedimentary basins because the parameters of such basins are not known in advance. Further, in the absence of additional information it becomes a uphill task to fit the theoretical gravity anomalies of a sedimentary basin with the observed ones by adjusting several depths to the interface in an interactive mode. In this context, Murthy and Rao (1989), Leão et al. (1996), Barbosa et al. (1997), Barbosa et al. (1999) developed methods using uniform density contrast to trace the basement interfaces from the observed gravity anomalies.

However, copious evidence exists to show that the density of sedimentary rocks varies with depth (Maxant, 1980; Hermes 1986; Moral *et al.* 2000; Nagihara and Hall,

2001, Chakravarthi, 2003, Chakravarthi, 2011) and hence using variable density models in the interpretation of gravity anomalies often ensures more reliable interpretations than the ones obtained using uniform density model. Ruotoistenmäki (1992), Zhou (2008), Zhou (2009) devised schemes to calculate the gravity effects of two-dimensional sources of arbitrary cross-sections using variable density contrast functions. Garcia-Abdeslem (1996) developed a code in Fortran to compute the gravity response of a vertical prism in which the density varies as a function of depth. Holstein (2003) presented formulas for the gravity potential, field, and field gradient tensor for a polyhedral target body of a spatially linear density medium and García-Abdeslem (2005) employed a cubic polynomial to describe the variation of density of sedimentary rocks with depth. The linear density function is more appropriate to describe the density variation of sediments at greater depths than at shallower depths (Chakravarthi, 2009a), whereas, the cubic polynomial fails to represent the actual density at greater depths (Chakravarthi and Sundararajan, 2006b, Chakravarthi, 2009b). Further, the enlisted forward modeling schemes also have limited practical application in analyzing the gravity anomalies of sedimentary basins.

A few automatic modeling techniques are in vogue to analyze the gravity anomalies of sedimentary basins using non-uniform density-depth models. For eg., Litinsky (1989) used a hyperbolic density function to calculate the thickness of sedimentary basins using the Bouguer slab formula. However, this method invariably incurs a considerable amount of error that is inversely proportional to the width of the basins (Chakravarthi and Sundararajan, 2004). The interpretation methods developed by Rao (1986), Rao (1990) using a quadratic density function would pose problems in automatic modeling and inversion of gravity anomalies because this density function deviates both in sign and magnitude from true density contrast at greater depths (Chakravarthi and Sundararajan, 2006b, Chakravarthi, 2009b). Based on the fact that exponential density function would provide geologically meaningful results if simple differential compaction is assumed to be the most important diagenetic process in the evolution of sedimentary basins (Cordell, 1973), and also realizing that no closed form analytical expression can be derived in the space domain using this density function, Murthy and Rao (1979) proposed an interpretation method, where each side of a polygon (used to describe the geometry of the basin) was sub-divided into a number of smaller segments and along each of which the density contrast was assumed to vary linearly with depth. This technique being effective consumes lot of time for modeling. Albeit, closed form analytical expression can be

derived for the gravity anomaly in the frequency domain, truncation errors would cause serious problems in modeling while transforming the anomalies from the frequency domain to the space domain in the methods of Codell (1973) and Chai and Hinge (1988), Rao and Rao (1999).

In this paper, we develop an automatic modeling technique in the space domain to analyze the gravity anomalies of sedimentary basins among which the density contrast varies exponentially with depth. The applicability and efficacy of the technique is demonstrated on both synthetic and real field gravity anomalies.

FORWARD MODELING – THEORETICAL CONSIDERATIONS

The Bott's (1960) method of profile gravity interpretation is extended to develop a strategy to analyze the gravity anomalies of sedimentary basins among which the density contrast decreases exponentially with depth (Cordell, 1973)

$$\Delta\rho(z) = \Delta\rho_0 e^{-\lambda z}, \quad (1)$$

where, $\Delta\rho_0$ is the density contrast observed at the ground surface and λ is a constant expressed in km^{-1} . These values can be estimated by fitting equation (1) to the known density contrast-depth data of sedimentary rocks.

Figure 1a shows the cross-section of a sedimentary basin and its approximation by a series of outcropping vertical prisms put in juxtaposition. In a Cartesian coordinate system, let $2T$ be the width of one such prism with z_T and z_B are the depths to the top and bottom of the prism respectively (Fig. 1b). Let the density contrast along the prism varies according to equation (1). The gravity anomaly at any point, $P(x,0)$, on the profile that runs along the x -axis can be expressed as,

$$\Delta g_{prism} = 2G\rho_0 \int_{z_T}^{z_B} e^{-\lambda z} \left[\tan^{-1} \frac{(x+T)}{z} - \tan^{-1} \frac{(x-T)}{z} \right] dz. \quad (2)$$

Here, G is the Universal Gravitational Constant.

The total gravity effect of the basin at any observation on the profile can be calculated as

$$\Delta g_{basin} = \sum_{i=1}^N \Delta g_{prism(i)}, \quad (3)$$

where, N is the number of prisms (observations). It is to be realized that equation (2) cannot be solved in the space domain in a closed form. Here, we solve this equation based on a numerical approach for its solution. Generally, numerical integration of a set of digitized values at equal intervals is convenient with the Simpson's rule. In case, the

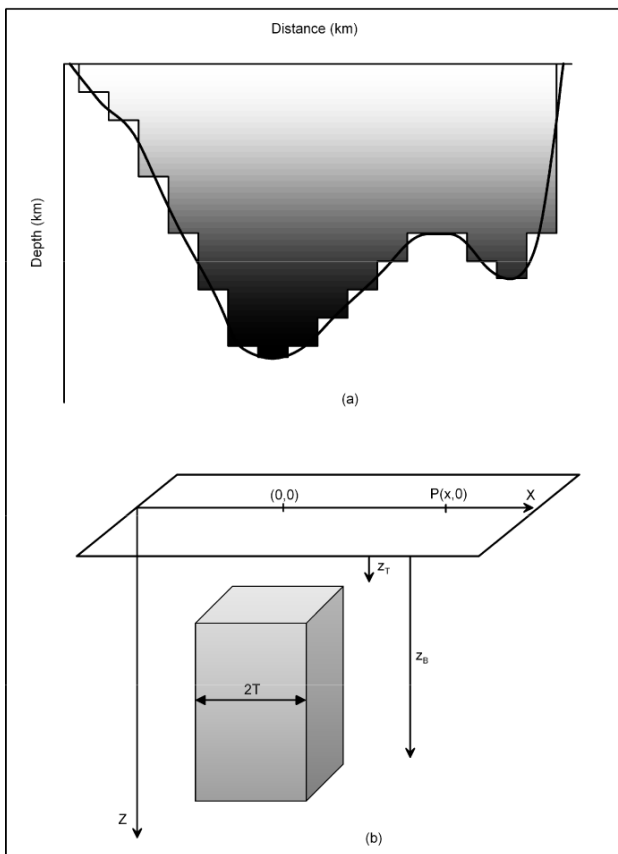


Fig.1. (a) Approximation of a sedimentary basin (solid line) by an ensemble of vertical prisms (step line). The shade within the basin from light to dark gray indicates increase in density of sediments with depth. **(b)** Geometry of a 2D vertical prism in Cartesian coordinate system.

sampled values show an unduly large variation between any pair of consecutive points then the Simpson's rule tends to be unreliable and in such a case it is convenient to assume an exponential variation in the digitized values between two consecutive points (Murthy, 1998). This approach has been adopted in the present case to obtain the numerical solution of equation (2).

To evaluate the accuracy of the proposed numerical method, the gravity effect produced by a vertical prism having dimensions $z_T = 0$ km, $z_B = 4$ km, $2T = 5$ km with uniform density contrast (-0.35 gm/cm³) was obtained from both the numerical integration of equation (2) and the analytic solution of equation (2) by Murthy (1998). The gravity response of the prism calculated from numerical and analytical solutions is shown in Fig.2. The maximum difference between the two anomalies is hardly 10^{-4} mGal, which demonstrates applicability of the numerical technique.

Further, to demonstrate the nature of gravity anomalies produced by a geological structure; two gravity profiles, one with exponential density contrast and the other using

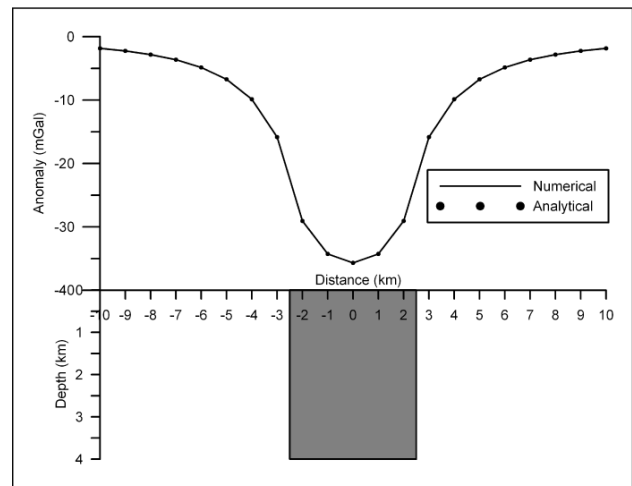


Fig.2. Gravity response of a vertical prism calculated by a numerical approach and by analytical solution.

uniform density, were generated (Fig.3a) on the plane, $z = 0$ km in the interval $x \in [-10$ km, 10 km] over a prismatic structure (Fig.3b) having parameters $z_T = 0.0$ km and $z_B = 4.0$ km, $2T = 5$ km. The exponential density function is defined with the constants $\Delta\rho_0 = -0.35$ gm/cm³ and $\lambda = 0.5$ km⁻¹, respectively. One can notice from Figure 3a that the maximum anomaly (absolute) produced by the structure with density model hardly exceeds half the maximum anomaly produced by the same structure with the uniform density model. It implies that sedimentary basins among which the density contrast varies exponentially with depth would generate only moderate gravity anomalies, and the fact that the present algorithm is also dependent on the magnitude of the anomalous field necessitates considering the exponential density model as a significant parameter in the interpretation for reliable results.

MODELING OF GRAVITY ANOMALIES

Modeling of gravity anomalies of a sedimentary basin tantamount to a mathematical exercise of estimating the depth values of the floor of a sedimentary basin from the measured gravity anomalies. The method of interpretation starts by initializing a sedimentary basin. It is presumed that at each observation, an infinite horizontal slab (Bouguer slab) in which, the density contrast varies according to equation (1) generates the corresponding observed gravity anomaly. The thickness of the Bouguer slab with exponential density contrast variation is given by (Cordell, 1973),

$$z_{Bou} = \frac{-1}{\lambda} \log \left(1 - \frac{\lambda g_{obs}}{2\pi G \rho_0} \right), \quad (4)$$

where, g_{obs} , is the observed gravity anomaly at any station.

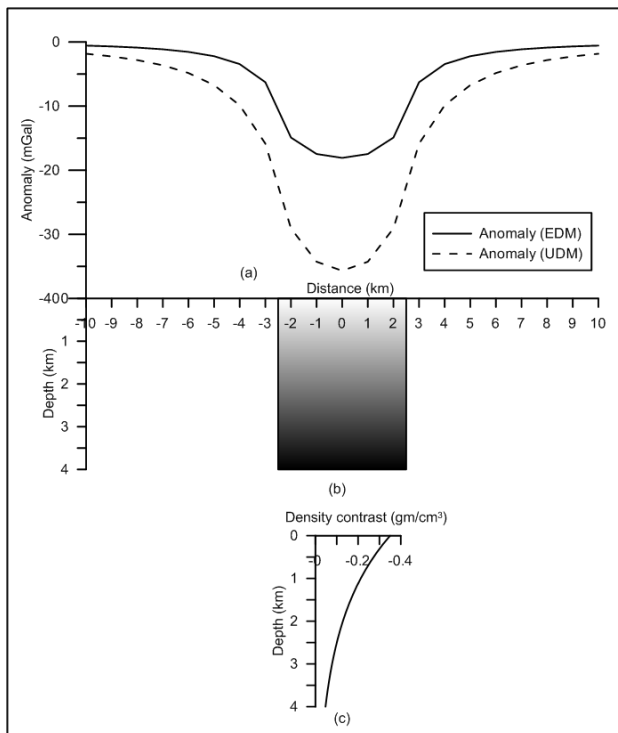


Fig.3. (a) Gravity anomalies with exponential and uniform density models, (b) Assumed structure, (c) exponential variation of density contrast with depth. The color gradation from light to dark gray within the prism indicates decrease in density contrast (absolute magnitude) with depth.

Using the initial depth estimates as obtained from equation (4), the theoretical gravity response of the basin can be calculated using equations (2) and (3). Since the initial depth estimates of a basin obtained from equation (4) are only approximate, the predicted/theoretical gravity anomalies obviously deviate from the measured ones and the difference between these anomalies can be used to improve the depth estimates of the prisms using the Newton’s forward difference approximation as,

$$z_{k+1}(x_i) = z_k(x_i) + \frac{g_{obs}(x_i) - g_{cal}(x_i)}{2\pi G \Delta \rho(z)}, i = 1, \dots, N, \tag{5}$$

where k stands for the number of iterations. The improved depth estimates are again used to compute the modeled gravity anomalies and the process repeats until one of the following conditions is satisfied.

- i) the specified number of iterations completed or,
- ii) the current value of the misfit, J, defined as the sum of the squares of the differences between the observed and modeled gravity anomalies, falls below a predefined allowable error or,

- iii) the current value of the misfit is larger than its previous value.

APPLICATIONS

Applicability and efficiency of the present modeling scheme are demonstrated by interpreting three gravity profiles; one over a synthetic model of a sedimentary basin and two real gravity anomaly profiles, one over the Chintalpudi sub-basin in India and the other over the San Jacinto graben, California. In all the examples, the observer locations are at the top of the topography.

Synthetic Example

Figure 4a shows 21 equispaced gravity anomaly observations (circles) in the interval $x \in [0 \text{ km}, 20 \text{ km}]$ produced by a simulated model of a sedimentary basin, whose geometry is shown in Figure 4b (step line in black). The assumed structure resembles a typical intracratonic rift basin formed by normal block faulting and filled with a thick sectioned sediments. A basement high at the centre is bounded on either side by steep vertical faults. The anomalies of the structure are generated presuming a surface density contrast of -0.45 gm/cm^3 with an exponent of 0.4 km^{-1} (Fig.4c). Negative gravity anomaly of the order of -25 mGal is observed at the 7th km on the profile (Figure 4a), adjacent to a relative gravity high observed over the basement high. The observed anomalies are subjected to modeling using the procedure outlined in the text. The initial structure of the basin estimated by the algorithm based on equation (4) is shown in Figure 4b as a dashed line and the corresponding theoretical gravity anomaly in Figure 4a as solid dots, respectively. The algorithm performed 396 iterations before it got terminated as the misfit falls below a predefined allowable error of 10^{-5} mGal . The misfit, J, reduced drastically from its initial value of 78.64 to 0.1 at the end of the 9th iteration and then gradually reaches to almost 0.0 at the end of the 396th iteration (Figure 5a). The modeled gravity anomalies subsequent to interpretation (shown in Figure 4a as a solid line in red) closely mimic the observed anomalies. Figure 5a shows the variation of misfit, J, against the iteration number.

The estimated structure (shown in Figure 4b as a step line in red) subsequent to modeling exactly mimics the assumed one over the length of the profile except at the centre, where the estimated depth deviates insignificantly from the assumed depth in the vicinity of the basement high (Figure 4b). The magnitude of error (%) between the assumed and estimated depths of the structure at each observation is shown in Figure 5b. It can be observed from

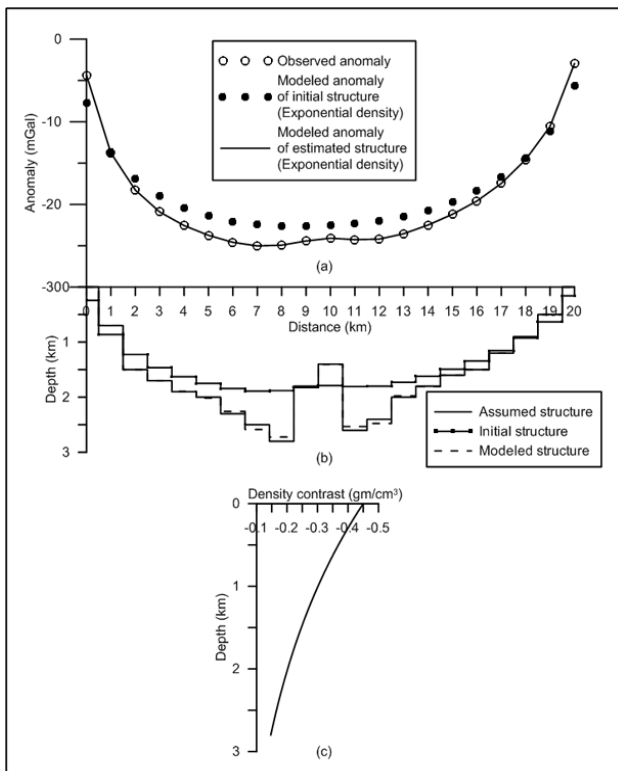


Fig.4. (a) Observed and theoretical gravity anomalies for initial and estimated depth structures of a synthetic basin model using exponential density function, (b) assumed, initial and estimated depth structures, (c) variation of density contrast with depth.

Figure 5b that the maximum error in depth between the assumed and estimated structure hardly exceeds 3%, which is negligible.

Furthermore, the gravity anomaly shown in Figure 4a is also interpreted assuming conventional uniform density model (-0.45 gm/cm^3). The initial depth structure and the corresponding gravity anomaly are shown in Figures 6a and 6b respectively. In this case, the algorithm performed 171 iterations before it terminates as the misfit function attains a value of almost zero from its initial value of 56.3 (Figure 5a). The modeled gravity anomaly and the derived depth structure were shown in Figures 6a and 6b. In this case, the estimated structure is grossly underestimated as much as 50% (Figure 5b). It can be observed from Figures 4a and 6a that the modeled gravity anomaly of the structure using exponential and uniform density equally fit the observed anomaly, however, the inverted structure with the exponential density function more or less mimics the actual one while it is not so with uniform density model.

Field Example – Chintalpudi Sub-basin

The proposed modeling technique is applied to interpret

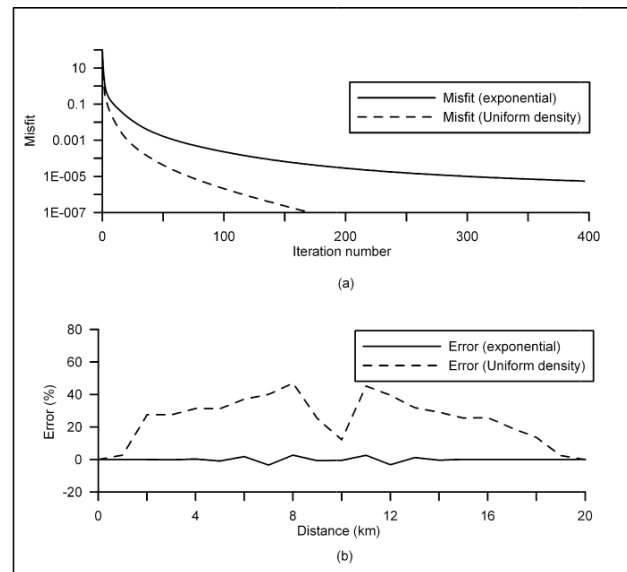


Fig.5. (a) Variation of misfit with iteration using exponential and uniform density models, (b) error between the assumed and estimated depth of the structure using exponential and uniform density models.

the observed gravity anomalies of the Chintalpudi sub-basin, India. The Pranhita-Godavari valley is a major NW-SE trending basin on the continental Precambrian platform. It largely follows the course of the Pranhita and Godavari rivers for over a strike length of 470 km. Based on the geology, structure and nature of the lithic fill, the Pranhita-Godavari valley is divided into the Godavari, Kothagudem, Chintalpudi and Krishna-Godavari sub-basins, respectively (Rao, 1982).

The Chintalpudi sub-basin represents the southeasterly continuation of the Kothagudem sub-basin of the Pranhita-

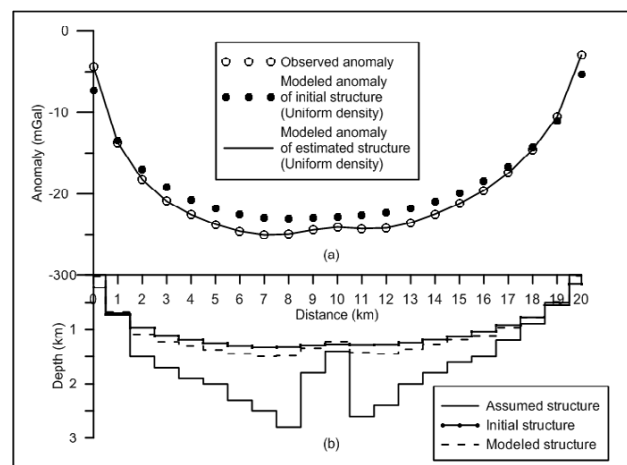


Fig.6. (a) Observed and theoretical gravity anomalies for initial and estimated depth structures using uniform density model, (b) assumed, initial and estimated depth structure.

Godavari valley and covers an area of 2500 sq km. In the sub-basin, Archaean gneisses form the basement for the Gondwana sequence, and the basin is of a younger generation, as evidenced by the absence of Barren Measure Formations over a major part of the area. The gravity anomaly map of the basin is shown in Figure 7a (Rao and Rao, 1999). The sub-basin is reflected with gravity minimum at the center and a maximum on either side over its shoulders. The Oil and Natural Gas Corporation Ltd. (ONGC), India, drilled a deep borehole within the basin and struck the basement rock (Archaean gneisses) at a depth of 2.935 km (Agarwal, 1995). The constants of exponential density function obtained by fitting equation (1) to the measured density contrast-depth data (Figure 7b) of the basin are given

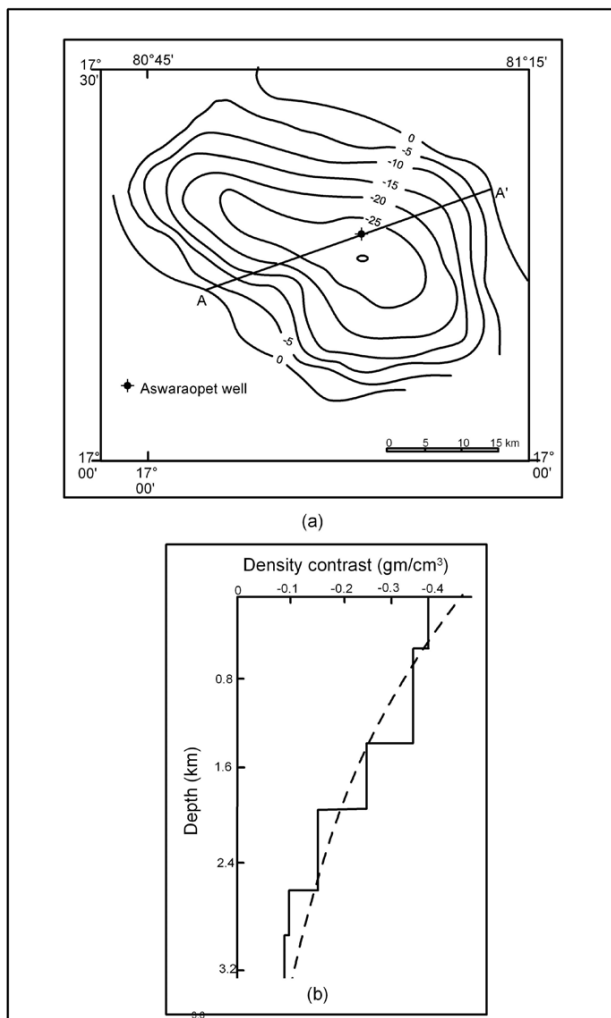


Fig.7. (a) Residual gravity anomaly, Chintalpudi subbasin, India (after Rao and Rao, 1999). Interpretation has been carried out along the profile AA', **(b)** measured density contrast-depth data (solid line) and fitted exponential density model (dashed line), Chintalpudi subbasin, India (modified after Rao and Rao, 1999).

as $\Delta\rho_0 = -0.4692 \text{ gm/cm}^3$ and $\lambda = 0.4078 \text{ km}^{-1}$, respectively (Rao and Rao, 1999).

For the present study, a gravity profile of 37.5 km length was constructed along a profile, AA', across the strike of the basin (Figures 7a) and subjected for modeling using both exponential and uniform density models. The algorithm took 88 and 23 iterations in each case respectively before it got terminated. The modeled gravity anomaly in each case is shown in Figure 8a along with the observed gravity anomaly. No significant changes in either depth of the structure or modeled gravity anomaly were noticed beyond the concluding iterations in both the cases. The interpreted depth structure of the basin in each case is shown in Figure 8b and the variation of misfit in Figure 8c respectively. The structure of the basin estimated by Rao and Rao (1999) along the same profile is also shown in Figure 8b for comparison. It can be observed from Figure 8b that the inferred structure by the present method using the exponential density function closely matches the one inferred by Rao and Rao (1999), which however is not repeated in case of uniform density model. Furthermore, the estimated depth of 3.1 km (using exponential density function) to the basement at the borehole location (Figure 8b) compares excellently with the drilling information. In this case, the error between the estimated and actual depth of the basement at the borehole location is about 5.6%, which is acceptable. In case of uniform density model, the basement depth is grossly underestimated (error in the estimated depth at the existing borehole is in excess of 45%), although the modeled gravity anomaly equally explains the observed anomaly as in the case of exponential density function (Figures 8b and 8a).

Field Example – San Jacinto Graben, California

The San Jacinto graben is bounded by two parallel branches of the San Jacinto fault, and has a northwesterly trend (Cordell, 1973). Country rock is a basement complex of pre-Tertiary schist and gneiss together with Cretaceous intrusive tonalities and granodiorites. Pliocene and Pleistocene detrital sedimentary rocks and Pleistocene and Holocene alluvium fill the graben, and the relatively lower density of this material accounts for the observed negative gravity anomaly. On the basis of seismic refraction data, Fett (1968) determined the depth of the basement in the center of the graben as 2.4 km. Cordell (1973) used an exponential density function defined with the constants $\Delta\rho_0 = -0.55 \text{ gm/cm}^3$ and $\lambda = 0.5 \text{ km}^{-1}$ (shown as dashed line in Fig. 9c) to simulate the derived density contrast-depth data of the graben (shown as solid line in Fig.9c) and adopted it to analyze the gravity anomalies of the basin (Fig.9a) for its basement structure (Fig.9b).

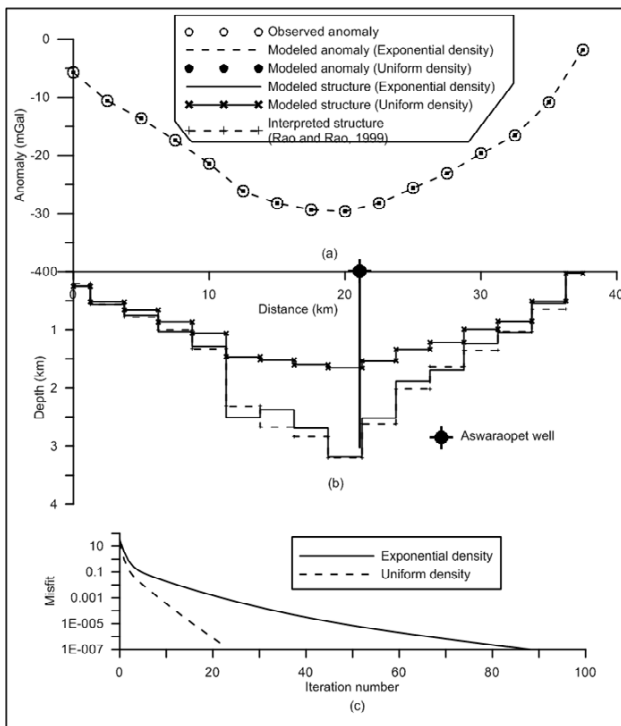


Fig.8. (a) Observed and modeled gravity anomalies using exponential and uniform density models, (b) estimated structures using exponential and uniform density models, (c) variation of misfit with iteration number, Chintalputi subbasin, India. Inferred depth structure by Rao and Rao (1999) is also shown in (b) for comparison.

For the present study, we digitize the observed gravity data of the graben at an interval of 0.322 km (Fig.9a) and subjected for modeling using both exponential and uniform density models following the procedure described in the text. For such a modeling, the algorithm performed 16 and 21 iterations respectively (Fig.9d). In case of exponential density model, the starting value of misfit was 252.8 and it drastically reduced to a value of 3.27 at the end of 9th iteration and then gradually to a value of 2.6 (Fig.9d). On the other hand, the misfit was reduced from its initial value of 190.7 to 0.17 at the end of the 21st iteration in case of uniform density model (Fig.9d). The modeled gravity anomaly in each case is shown in Fig.9a and the corresponding estimated depth structure in Fig.9b respectively. The structure derived by Cordell (1973) is also shown in the Fig.9b for comparison. The maximum depth to the basement obtained from the present method is 2.62 km. Fett (1968) and Cordell (1973) concluded that the maximum thickness of sediments within the graben is at least 2.44 km. Further, one can notice from Figure 9b that the estimated structure by the present method using the exponential density model is closely matches with the one

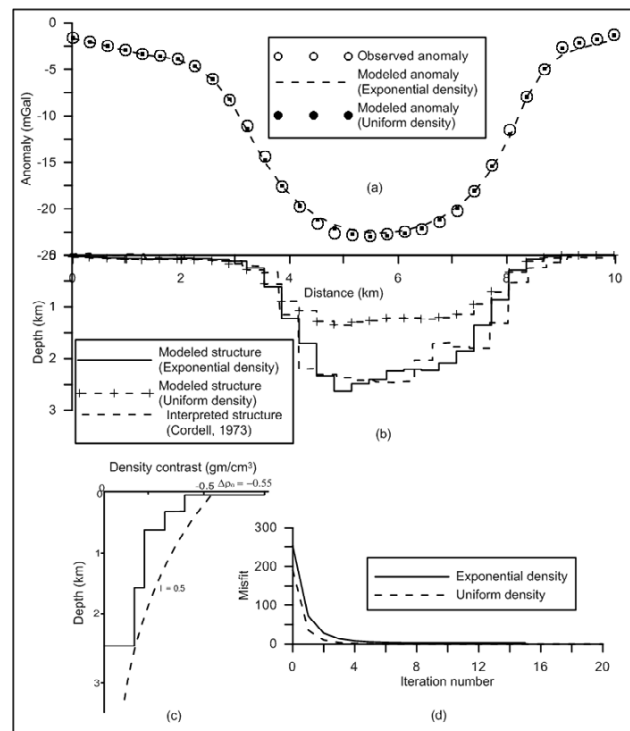


Fig.9. (a) Observed and modeled gravity anomalies using exponential and uniform density models, (b) estimated structures using exponential and uniform density models, (c) predicted density contrast-depth data (solid line) by Fett (1968) and fitted exponential density model (dashed line) by Cordell (1973), (d) variation of Misfit with iteration number, San Jacinto graben, California. Inferred depth structure by Cordell (1973) is also shown in (b) for comparison.

derived by Cordell. In case of uniform density model, the maximum depth to the basement obtained was 1.35 km, which is not consistent with the known geological information of the basin.

CONCLUSIONS

The major conclusions and salient features of the investigation are mainly on the following lines

1. Novelty in the methodology,
2. Efficiency and applicability of modeling.

A new modeling scheme is developed to analyze the gravity anomalies of sedimentary basins by means of growing bodies and exponential density contrast-depth variations. Although, it is well known that no closed form solution exists in the space domain for the gravity anomalies of geophysical geometries using an exponential density function, a new strategy has been formulated in the space domain to realize forward modeling by judiciously

combining both analytical and numerical approaches.

The efficacy of the method is that it is fully automatic in the sense that it generates initial structures of sedimentary basins from observed gravity anomalies, and improves the structures based on the differences between the observed and modeled gravity anomalies until the modeled anomalies mimic the observed ones. The applicability and validity of this modeling technique is demonstrated on both synthetic and real field gravity anomalies. Modeling of gravity anomalies of sedimentary basins with exponential density function remarkably agree with the assumed parameters in the case of a synthetic structure. Further, the estimated basement depths of the Chintalpudi sub-basin in India and San Jacinto graben in California from gravity modeling

using the present method with an exponential density function excellently coincide with drilling/available depths. On the other hand, in almost all cases, when uniform density model is implemented it had resulted in inaccurate depth structures, implying that uniform density model is inappropriate in such applications. In short, it is concluded that the proposed algorithm is simple, elegant besides being effective.

Acknowledgements: The authors sincerely thank anonymous reviewers for their critical reviews and feedback to revise the manuscript as presented. Director, Centre for Earth & Space Sciences is acknowledged for providing facilities to carry out the work.

References

- AGARWAL, B.P. (1995) Hydrocarbon prospects of the Pranhita-Godavari graben, India. *Proc. Petrotech*, v.95, pp.115–121.
- BARBOSA, V.C.F., SILVA, J.B.C. and MEDEIROS, W.E. (1997) Gravity inversion of basement relief using approximate equality constraints on depths. *Geophysics*, v.62(6), pp.1745–1757.
- BARBOSA, V.C.F., SILVA, J.B.C. and MEDEIROS, W.E. (1999) Gravity inversion of a discontinuous relief stabilized by weighted smoothness constraints on depth. *Geophysics*, v.64(5), pp.1429–1437.
- BLAKELY, R.J. (1995) *Potential Theory in Gravity and Magnetic Applications*. Cambridge Univ. Press, Cambridge, UK, 464p.
- BOTT, M.H.P. (1960) The use of rapid digital computing methods for direct gravity interpretation of sedimentary basins. *Geophys. Jour. Royal Astron. Soc*, v.3(1), pp.63–67.
- CHAI, Y. and HINZE, W.J. (1988) Gravity inversion of an interface above, which the density contrast varies exponentially with depth. *Geophysics*, v.53(6), pp.837–845.
- CHAKRAVARTHI, V. (2003) Digitally implemented method for automatic optimization of gravity fields obtained from three-dimensional density interfaces using depth dependent density. US Patent 6,615,139.
- CHAKRAVARTHI, V. (2009a) Gravity anomalies of pull-apart basins having finite strike length with depth dependent density: A ridge regression inversion. *Near Surface Geophysics*, v.7, pp.217–226.
- CHAKRAVARTHI, V. (2009b) Automatic gravity inversion for simultaneous estimation of model parameters and regional gravity background: an application to 2D pull-apart basins. *Curr. Sci.*, v.96(10), pp.1349–1360.
- CHAKRAVARTHI, V. (2011) Automatic gravity optimization of 2.5D strike slip fault sources with analytically defined fault planes and depth dependent density. *Geophysics*, v.76(2), pp.121–131.
- CHAKRAVARTHI, V. and SUNDARARAJAN, N. (2004) Ridge regression algorithm for gravity inversion of fault structures with variable density. *Geophysics*, v. 69, pp.1394–1404.
- CHAKRAVARTHI, V. and SUNDARARAJAN, N. (2006a) Gravity anomalies of 2.5-D multiple prismatic structures with variable density: A Marquardt inversion. *Pure and Applied Geophysics*, v.163, pp.229–242.
- CHAKRAVARTHI, V. and SUNDARARAJAN, N. (2006b) Discussion on “The gravitational attraction of a right rectangular prism with density varying with depth following a cubic polynomial” by Juan Garcia-Abdeslem (November-December 2005, *Geophysics*, pp.j39-j42), *Geophysics*, v.71, pp.X17–X19.
- CORDELL, L. (1973) Gravity analysis using an exponential density-depth function-San Jacinto Graben, California. *Geophysics*, v.38(4), pp.684–690.
- FETT, J.D. (1968) *Geophysical investigation of the San Jacinto Valley, Riverside County, California*: Unpublished thesis, University of California at Riverside, 87p.
- GARCIA-ABDESLEM, J. (1996) GL2D: A Fortran program to compute the gravity anomaly of a 2-d prism where density varies as a function of depth. *Computers & Geosciences*, v.22(7), pp.823–826.
- GARCIA-ABDESLEM, J. (2005) The gravitational attraction of a right rectangular prism with density varying with depth following a cubic polynomial. *Geophysics*, v.70, pp.j39-j42.
- HERMES, H.J. (1986) Calculation of pre-Zechstein Bouguer anomaly in northwest Germany. *First Break*, v.4, pp.13–22.
- HOLSTEIN, H. (2003) Gravimagnetic anomaly formulas for polyhedra of spatially linear media. *Geophysics*, v.68, pp.157–167.
- LEÃO, J.W.D., MENEZES, P.T.L., BELTRÃO, J.F. and SILVA, J.B.C. (1996) Gravity inversion of basement relief constrained by the knowledge of depth at isolated points. *Geophysics*, v.61(6), pp.1702–1714.
- LITINSKY, V.A. (1989) Concept of effective density: key to gravity depth determinations for sedimentary basins. *Geophysics*, v.54(11), pp.1474–1482.
- MAXANT, J. (1980) Variation of density with rock type, depth, and formation in the Western Canada basin from density logs. *Geophysics*, v.45(6), pp.1061–1076.

- MORAL, C.R., GÚMEZ ORTIZ, D. and TEJERO, R. (2000) Spectral analysis and gravity modelling of the Almazán basin (Central Spain). *Jour. Geol. Soc. Spain*, v.13, pp.131-142.
- MURTHY, I.V.R. (1998) Gravity and magnetic interpretation in exploration geophysics. Geological Society of India, Bangalore, 363p.
- MURTHY, I.V.R. and RAO, D.B. (1979) Gravity anomalies of two-dimensional bodies of irregular cross-section with density contrast varying with depth. *Geophysics*, v.44(9), pp.1525-1530.
- MURTHY, I.V.R. and RAO, S.J. (1989) A Fortran 77 program for inverting gravity anomalies of two-dimensional basement structures. *Computers & geosciences*, v.15(7), pp.1149-1156.
- NAGIHARA, S. and HALL, S.A. (2001) Three-dimensional gravity inversion using simulated annealing: constraints on the diapiric roots of allochthonous salt structures. *Geophysics*, v.66, pp.1438-1449.
- RAO, C.S.R. (1982) Coal resources of Tamilnadu, Andhra Pradesh, Orissa and Maharashtra. *Bull. Geol Surv. India*, v.2, pp.1-103.
- RAO, D.B. (1986) Modeling of sedimentary basins from gravity anomalies with variable density contrast. *Geophys. Jour. Royal Astron. Soc.*, v.84(1), pp.207-212.
- RAO, D.B. (1990) Analysis of gravity anomalies of sedimentary basins by an asymmetrical trapezoidal model with quadratic density function. *Geophysics*, v.55, pp.226-231.
- RAO, D.B. and RAO, C.P.V.N.J.M. (1999) Two-dimensional interpretation of gravity anomalies over sedimentary basins with an exponential decrease in density contrast with depth. *Proc. Indian Acad. Sci. (Earth Planet. Sci.)*, v.108(2), pp.99-106.
- RUOTOISTENMÄKI, T. (1992) The gravity anomaly of two-dimensional source with continuous density distribution bounded by continuous surfaces. *Geophysics*, v.57(4), pp.623-628.
- SINGH, B. and GUPTASARMA, D. (2001) New method for fast computation of gravity and magnetic anomalies from arbitrary polyhedral. *Geophysics*, v.66, pp.521-526.
- TALWANI, M., WORZEL, J. and LADISMAN, M. (1959) Rapid gravity computations for two dimensional bodies with application to the Mendocino submarine fracture zone. *Jour. Geophys. Res.*, v.64(1), pp.49-59.
- WON, I.J. and BEVIS, M. (1987) Computing the gravitational and magnetic anomalies due to a polygon: Algorithms and Fortran subroutines., *Geophysics*, v.52, pp.232-238.
- ZHOU, X. (2008) Two-dimensional (2D) vector gravity potential and general line integrals for gravity anomaly due to 2D masses of depth-dependent density contrast. *Geophysics*, v.73, pp.143-150.
- ZHOU, X. (2009) General line integrals for gravity anomalies of irregular two-dimensional (2D) masses with horizontally- and vertically-dependent density contrast. *Geophysics*, v.74, pp.11-17.

(Received: 1 June 2012; Revised form accepted: 9 September 2012)